ARTICLE

Exonic Deletions in *AUTS2* Cause a Syndromic Form of Intellectual Disability and Suggest a Critical Role for the C Terminus

Gea Beunders,[1,37] Els Voorhoeve,[1,37] Christelle Golzio,[2] Luba M. Pardo,[1] Jill A. Rosenfeld,[3] Michael E. Talkowski,[4,5] Ingrid Simonic,[6] Anath C. Lionel,[7,8] Sarah Vergult,[9] Robert E. Pyatt,[10,11] Jiddeke van de Kamp,[1] Aggie Nieuwint,[1] Marjan M. Weiss,[1] Patrizia Rizzu,[1] Lucilla E.N.I. Verwer,[1] Rosalina M.L. van Spaendonk,[1] Yiping Shen,[4,12,13] Bai-lin Wu,[12,14] Tingting Yu,[12,13] Yongguo Yu,[12,13] Colby Chiang,[4] James F. Gusella,[4,5] Amelia M. Lindgren,[15,16] Cynthia C. Morton,[5,15,16] Ellen van Binsbergen,[17] Saskia Bulk,[17] Els van Rossem,[18] Olivier Vanakker,[9] Ruth Armstrong,[6] Soo-Mi Park,[6] Lynn Greenhalgh,[19] Una Maye,[19] Nicholas J. Neill,[3] Kristin M. Abbott,[6] Susan Sell,[20] Roger Ladda,[20] Darren M. Farber,[21] Patricia I. Bader,[22] Tom Cushing,[23] Joanne M. Drautz,[23] Laura Konczal,[24] Patricia Nash,[25] Emily de Los Reyes,[26] Melissa T. Carter,[27] Elizabeth Hopkins,[28] Christian R. Marshall,[7,8] Lucy R. Osborne,[29] Karen W. Gripp,[28] Devon Lamb Thrush,[10,30] Sayaka Hashimoto,[10] Julie M. Gastier-Foster,[10,11] Caroline Astbury,[10,11] Bauke Ylstra,[31] Hanne Meijers-Heijboer,[1] Danielle Posthuma,[1,32,33] Björn Menten,[9] Geert Mortier,[34] Stephen W. Scherer,[7,8] Evan E. Eichler,[35] Santhosh Girirajan,[35,36] Nicholas Katsanis,[2] Alexander J. Groffen,[1,32] and Erik A. Sistermans[1,*]

Genomic rearrangements involving *AUTS2* (7q11.22) are associated with autism and intellectual disability (ID), although evidence for causality is limited. By combining the results of diagnostic testing of 49,684 individuals, we identified 24 microdeletions that affect at least one exon of *AUTS2*, as well as one translocation and one inversion each with a breakpoint within the *AUTS2* locus. Comparison of 17 well-characterized individuals enabled identification of a variable syndromic phenotype including ID, autism, short stature, microcephaly, cerebral palsy, and facial dysmorphisms. The dysmorphic features were more pronounced in persons with 3′ *AUTS2* deletions. This part of the gene is shown to encode a C-terminal isoform (with an alternative transcription start site) expressed in the human brain. Consistent with our genetic data, suppression of *auts2* in zebrafish embryos caused microcephaly that could be rescued by either the full-length or the C-terminal isoform of AUTS2. Our observations demonstrate a causal role of AUTS2 in neurocognitive disorders, establish a hitherto unappreciated syndromic phenotype at this locus, and show how transcriptional complexity can underpin human pathology. The zebrafish model provides a valuable tool for investigating the etiology of AUTS2 syndrome and facilitating gene-function analysis in the future.

[1]Department of Clinical Genetics, VU University Medical Center, Amsterdam 1007 MB, The Netherlands; [2]Center for Human Disease Modeling, Department of Cell Biology, Duke University Medical Center, Durham, NC 27710, USA; [3]Signature Genomic Laboratories, Perkin Elmer, Spokane, WA 99207, USA; [4]Center for Human Genetic Research, Massachusetts General Hospital, affiliated with Departments of Genetics and Neurology, Harvard Medical School, Harvard University, Boston, MA 02114, USA; [5]Program in Medical and Population Genetics, Broad Institute, Cambridge, MA 02142, USA; [6]East Anglian Medical Genetics Service, Addenbrooke's Hospital, Cambridge University Hospitals, National Health Service Foundation Trust, Cambridge, CB2 0QQ, UK; [7]The Centre for Applied Genomics and Program in Genetics and Genome Biology, The Hospital for Sick Children, Toronto, ON M5G 1L7, Canada; [8]Department of Molecular Genetics and the McLaughlin Centre, University of Toronto, Toronto, ON M5S 1A1, Canada; [9]Center for Medical Genetics, University Hospital Ghent, Ghent 9000, Belgium; [10]Pathology and Laboratory Medicine, Nationwide Children's Hospital, Columbus, OH 43205, USA; [11]Department of Pathology, The Ohio State University, Columbus, OH 43210, USA; [12]Department of Laboratory Medicine, Boston Children's Hospital, Boston, MA 02114, USA; [13]Shanghai Children's Medical Center, Shanghai Jiaotong University School of Medicine, Shanghai 200025, China; [14]Children's Hospital and Institutes of Biomedical Science, Fudan University, Shanghai 200032, China; [15]Department of Pathology, Brigham and Women's Hospital, Boston, MA 02115, USA; [16]Department of Obstetrics, Gynecology, and Reproductive Biology, Harvard Medical School, Boston, MA 02115, USA; [17]Department of Medical Genetics, University Medical Center Utrecht, Utrecht 3508 AB, The Netherlands; [18]Onze-Lieve-Vrouwe Ziekenhuis, Aalst 9300, Belgium; [19]Clinical Genetics, Royal Liverpool Children's Hospital, Eaton Road, Alder Hey, Liverpool L12 2AP, Great Britain; [20]Penn State Milton S. Hershey Medical Center, Hershey, PA 17033, USA; [21]Department of Neurology, University of Louisville, Louisville, KY 40222, USA; [22]Northeast Indiana Genetic Counseling Center, Ft. Wayne, IN 46804, USA; [23]Pediatric Genetics Division, Department of Pediatrics, University of New Mexico, Albuquerque, NM 87131, USA; [24]University Hospitals, Case Western Reserve University, Cleveland, OH 44106, USA; [25]Department of Behavioral Pediatrics, Nationwide Children's Hospital, Columbus, OH 43205, USA; [26]Department of Pediatrics and Neurology, The Ohio State University, Columbus, OH 43210, USA; [27]Division of Clinical and Metabolic Genetics, The Hospital for Sick Children, Toronto, ON M5G 1X8, Canada; [28]Division of Medical Genetics, Alfred I. duPont Hospital for Children, Wilmington, DE 19803, USA; [29]Departments of Medicine and Molecular Genetics, University of Toronto, Toronto, ON M5S 1A8, Canada; [30]Department of Pediatrics, The Ohio State University, Columbus, OH 43210, USA; [31]Department of Pathology, VU University Medical Center, Amsterdam 1007 MB, The Netherlands; [32]Department of Functional Genomics, Center for Neurogenomics and Cognitive Research, Neuroscience Campus Amsterdam, VU University, Amsterdam 1081 HV, The Netherlands; [33]Department of Child and Adolescent Psychiatry, Erasmus University Rotterdam, Rotterdam 3000 CB, The Netherlands; [34]Department of Medical Genetics, Antwerp University, Edegem 2650, Belgium; [35]Department of Genome Sciences and Howard Hughes Medical Institute, University of Washington, Seattle, WA 98195, USA; [36]Department of Biochemistry and Molecular Biology Department of Anthropology, Pennsylvania State University, Pennsylvania, PA 16803, USA
[37]These authors contributed equally to this work
*Correspondence: e.sistermans@vumc.nl
http://dx.doi.org/10.1016/j.ajhg.2012.12.011.

Introduction

Neurodevelopmental disorders, including intellectual disability (ID) and autism, have a strong genetic component, but only a few of the underlying genes have been identified. Candidate-gene discovery has accelerated in recent years by the implementation of high-resolution genomic arrays. However, detected copy-number variants (CNVs) often either encompass multiple genes or are too rare to provide causal evidence for a particular candidate transcript. Autism susceptibility candidate 2 (*AUTS2*), located on 7q11.22 (MIM 607270), represents such an ID candidate with inconclusive evidence for causality.

AUTS2 was first identified as a candidate for neurocognitive defects because a translocation-breakpoint analysis in twins with autism, developmental delay, and epilepsy showed that one of the breakpoints disrupted *AUTS2*.[1] Besides the twins, seven additional cases have now been reported to have a disrupted *AUTS2* coding region: four individuals with a translocation breakpoint,[2,3] one with an inversion breakpoint disrupting *AUTS2*,[2–4] and two with intragenic deletions.[2,5] These individuals manifested ID and developmental delay (all nine), dysmorphic features (six), autism (four), and skeletal abnormalities (three). This overview does not include persons with intronic deletions in *AUTS2* because the functional significance of such intronic variation is unclear.[6]

Complicating the candidacy of this locus, some of the genomic rearrangements affecting *AUTS2* disrupt other genes as well. A combination of cytogenetic and sequencing studies suggested that *CNTNAP2* (7q35) might be causal in an individual with a 7q inversion disrupting *AUTS2* and *CNTNAP2* (MIM 604569);[4] likewise, for three larger multigenic de novo deletions (in the DECIPHER database) encompassing *AUTS2*, it is unclear whether the disruption of *AUTS2* alone drives the phenotype.[7] The data presented by Nagamani et al.[5] on two individuals with intragenic deletions suggest that deletions in *AUTS2* alone might be pathogenic. However, the number of affected individuals was too small to exclude the role of other genes or to delineate a phenotype.[5] Here, we present direct evidence from both clinical and genetic data and animal studies for the causal relation of *AUTS2* with an ID syndrome and delineate the associated phenotype. Furthermore, we provide evidence that functional elements in the C terminus of AUTS2 are major contributors to both the neurodevelopmental and craniofacial phenotypes of individuals with C-terminal deletions or rearrangements at this locus.

Subjects and Methods

Subjects

Routine diagnostic array comparative genomic hybridization (CGH) was performed for ID and/or multiple congenital anomalies (MCAs) for a total of 49,684 individuals across ten diagnostic centers in The Netherlands, Belgium, Great Britain, the United States, and Canada (each center used their standard diagnostic platform; in total, six analogous platforms were used). In some of these individuals, karyotyping was also performed. From this cohort, we selected all individuals with a deletion involving *AUTS2*, as well as one person with a translocation and another person with an inversion in which one of the breakpoints was in *AUTS2*. To map the region further and to delineate the associated phenotypes, we obtained peripheral-blood samples and collected clinical information through either medical letters or a data sheet filled in by the referring physicians with approval of the local medical ethical committee. Results were confirmed with different methods (high-density array, multiplex ligation-dependent probe amplification [MLPA], and fluorescence in situ hybridization [FISH]) depending on the laboratory (see Tables S1, S2, and S3, available online). Exact breakpoint delineation of the translocation with one breakpoint in 7q11.22 was performed with FISH, and the inversion was characterized with whole-genome sequencing, as previously described.[8–10] Informed consent was obtained from parents or caregivers as appropriate, and specific consent for publishing photographs was obtained from all individuals whose photographs are shown here. Institutional approval of the local medical ethical committee was obtained as well. Individuals with a confirmed exonic deletion or a genomic rearrangement involving *AUTS2* and available clinical data were included for phenotypic studies.

Controls

To assess the frequency of *AUTS2* deletions within a large general population, we analyzed CNV data of 16,784 subjects from several control groups. A total of 4,783 DNA samples from the Wellcome Trust Case Control Consortium 2 (WTCCC2) were analyzed with a SNP array. This control group included individuals who had been nationally ascertained and regarded as healthy from the 1958 Birth Cohort and the UK Blood Service collection (October 26, 2011).[11] Further control CNV data from 8,329 cell-line- and blood-derived controls were obtained primarily from genome-wide association studies of nonneurological phenotypes. Because these included 2,090 controls from the UK Blood Service collection, this set added only 6,239 unique controls. Although these data were not ascertained specifically for neurological disorders, they consist of adult individuals who provided informed consent as described previously.[12] In addition, publicly available data from HapMap phase 3 (October 26, 2011), which consists of 1,056 healthy controls from 11 different populations, were checked for deletions involving *AUTS2*.[13] CNV data were available from the following four control sets: The Ottawa Heart Institute (OHI) controls (n = 1,234) from Canada, POPGEN controls (n = 1,123) from Germany, SAGE controls (n = 1,287) from the United States, and the Low-Lands-Consortium controls (n = 981) from The Netherlands.[13–15] See Table S4 for details on all cohorts and the array platforms used. The array platforms used for controls have the same or a comparable resolution as the platforms used for cases. The number of deletions found in the cases was compared to that in the controls with a Fisher's exact test.

Genotype-Phenotype Correlations

We received clinical data from 17 individuals and 4 family members carrying an exonic *AUTS2* disruption. We used these individuals to identify features that occurred in at least two unrelated individuals, i.e., features with a minimal frequency of 10%.

A recent systematic review of Oeseburg et al.[16] showed that in a general ID cohort, the most frequent additional health conditions (epilepsy and cerebral palsy) are as frequent as 20%, but the remainder of the comorbid clinical features (including autism and a congenital malformation in general) are seen in less than 10%.[16] Therefore, a frequency of 10% for a specific feature in this AUTS2 cohort is an enrichment compared to ID cases in general. These recurrent features were scored for all individuals and family members carrying the familial deletion, and asymmetrically occurring features were counted as positive. The sum of positive features was counted for each individual and was defined as his or her individual AUTS2 syndrome severity score.

Because deletions or genomic rearrangements affecting the 3′ end of the *AUTS2* coding sequence seem to be associated with a more severe phenotype, persons with exonic deletions were categorized in two groups depending on whether the deletion disrupted the highly conserved *AUTS2* segment (containing exons 9–19) that is also encoded by the alternative 3′ transcript (see Alternative Transcription Start Sites below and the Results). We used a Kolmogorov-Smirnov test to test whether the corresponding AUTS2 syndrome severity scores for these two groups differed significantly.

Alternative Transcription Start Sites

To search for an explanation for the observed genotype-phenotype trend, we first determined the evolutionary conservation of human *AUTS2* exonic sequences. We used the following species for comparison: gorilla (*Gorilla gorilla*; gorGor3), macaque (*Macaca mulatta*; Mmul_1), dog (*Canis familiaris*; Broadd2), cow (*Bos taurus*; Btau_4.0), pig (*Sus scrofa*; Sscrofa9), mouse (*Mus musculus*; NCBIM37), chicken (*Gallus gallus*; Washuc2), clawed frog (*Xenopus tropicalis*; JGI_4.2), and zebrafish (*Danio rerio*; Zf9). Accession numbers of protein sequences are ENSGGOP00000011519, ENSMMUP00000023254, ENSBTAP00000002697, ENSSSCP00000008253, ENSCAFP00000016549, ENSMUSP00000062515, ENSGALP00000001729, ENSXETP00000007747, and ENSDARP00000073379. Two different methods were used. We first aligned the predicted protein of the longest isoform in humans to the predicted amino acid sequences of the orthologous species by using MUSCLE v.3.8 software.[17] For that purpose, we downloaded sequences from the latest builds from Ensembl. Then, to detect similarity in nonannotated or noncoding genomic DNA, we used the tblastn algorithm (see Web Resources) with the human amino acid sequence as query.[18] The degree of homology was calculated as the percentage of identical amino acids.

Second, we searched for putative alternative transcription start sites (TSSs) that were associated with a shorter 3′ isoform in the human brain. We used mRNA from the caudate nucleus and the medial frontal gyrus from one donor provided by the Dutch Brain Bank and performed a replication experiment by the same procedure on a mRNA sample from the medial frontal gyrus of a second donor. Rapid amplification of 5′ cDNA ends (5′ RACE) was performed with the Ambion FirstChoice RLM-RACE kit according to the manufacturer's instructions. Nested PCR amplification was performed with 5′-ATGTCTTCGGCTGAAATGCT-3′ as the outer *AUTS2*-specific reverse primer and 5′-GGAAGAGACTGTGCCGGTAG-3′ as the inner primer (Figures S1A and S1B).

Knockdown and Rescue Experiments in Zebrafish Embryos

To investigate the role of AUTS2 in the regulation of head size, neuronal development, and morphology in general, we performed zebrafish knockdown experiments. Zebrafish (*Danio rerio*) embryos were raised and maintained as described.[19] Splice-blocker morpholinos (MOs) against the *AUTS2* ortholog *auts2* were designed and obtained from Gene Tools (Table S5). We injected 1 nl of diluted MOs (4.5 ng for the 5′ MO targeting the exon 2 donor splice and 6 ng for the 3′ MO targeting the exon 10 donor splice) and/or 100 pg of mRNA into wild-type zebrafish embryos at the 1- to 2-cell stage (n = 50–100 embryos per injection dose) and performed RT-PCR to measure efficiency of the splice blocking. Injected embryos were scored visually at 3 days postfertilization (dpf) and classified as normal or microcephalic on the basis of the relative head size compared with that of age-matched controls from the same clutch. For rescue experiments, the human wild-type mRNAs (full-length or short transcript [GenBank accession numbers JQ670866 and JQ670867, respectively]) were cloned into the pCS2 vector and transcribed in vitro with the SP6 Message Machine kit (Ambion); 100 pg of the human wild-type mRNAs were coinjected with the MOs. All experiments were repeated three times and evaluated statistically with a Student's t test. Alcian-blue staining of cartilaginous structures was performed for investigating the morphology of the head. Zebrafish embryos were fixed with 4% paraformaldehyde (PFA), and the cartilage structures were visualized by Alcian-blue staining according to an established protocol.[20] Further, whole-mount immunostainings with either HuC/D (postmitotic neurons) or phosphohistone H3 (proliferating cells) were performed for investigating neuronal development and head-size regulation at a cellular level. Embryos were fixed in 4% PFA overnight and stored in 100% methanol at −20°C. After rehydration in PBS, PFA-fixed embryos were washed in immunofluorescence (IF) buffer (0.1% Tween-20 and 1% BSA in PBS 1×) for 10 min at room temperature. The embryos were incubated in the blocking buffer (10% FBS and 1% BSA in PBS 1×) for 1 hr at room temperature. After two washes in IF buffer for 10 min each, embryos were incubated in the first antibody solution, 1:750 anti-histone H3 (ser10)-R (sc-8656-R, Santa Cruz) or 1:1,000 anti-HuC/D (A21271, Invitrogen), in blocking solution overnight at 4°C. After two washes in IF buffer for 10 min each, embryos were incubated in the secondary antibody solution, 1:1,000 Alexa Fluor donkey anti-rabbit IgG and Alexa Fluor goat anti-mouse IgG (A21207, A11001, Invitrogen), in blocking solution for 1 hr at room temperature. Staining was quantified by the counting of positive cells in defined regions of the head and with ImageJ software.

Results

Genotypes

To assess the candidacy of *AUTS2* in cognitive impairment in humans, we examined the *AUTS2* region in 49,684 individuals with ID and/or MCAs by using array CGH and/or karyotyping. We identified 44 deletions encompassing at least part of *AUTS2* and a maximum of two other genes (*WBSCR17* and *CALN1* [MIM 607176]), and conventional karyotyping revealed one translocation and one inversion each with one breakpoint in *AUTS2* (Table S1). *AUTS2*-encompassing duplications found in this cohort were not included in this study because the functional relevance of these lesions is unclear. Twenty-four deletions were found to include at least one *AUTS2* exon, whereas another 17 did not. For the remaining three deletions, it was

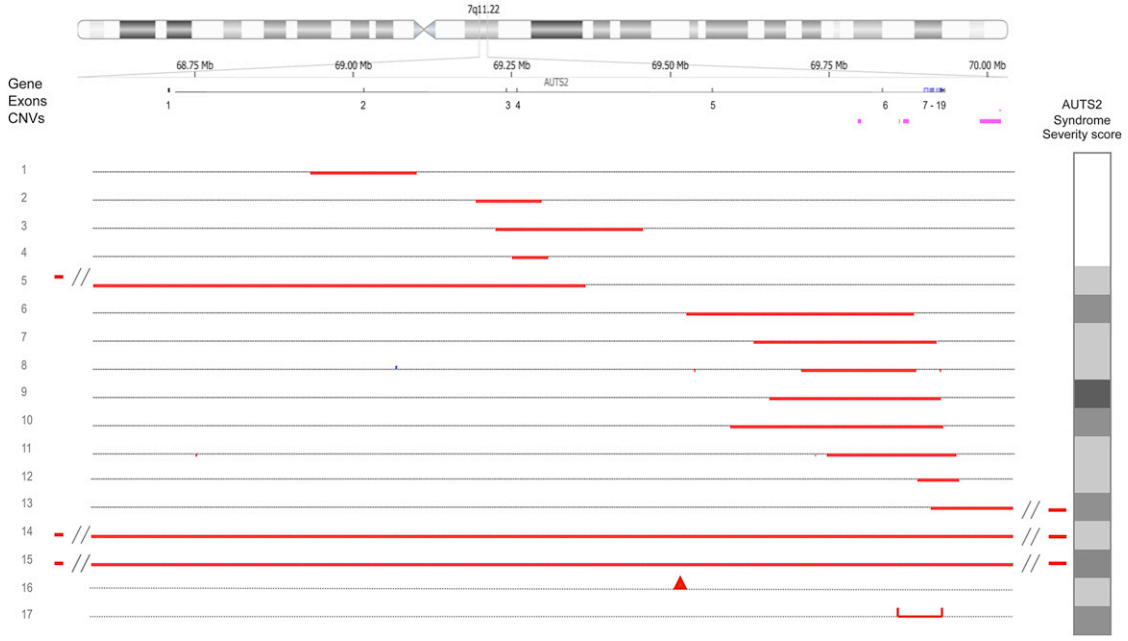

Figure 1. Overview of *AUTS2* Aberrations in the Probands
The location of the deletions is indicated by the red bars, the inversion breakpoint is indicated by an arrowhead, and the translocation breakpoint area is indicated by the red horizontal bracket. CNVs extracted from the Database of Genomic Variants are in purple (CNVs found in bacterial-artificial-chromosome studies are not included). The AUTS2 syndrome severity score of the probands is shown on the right. Darker shades indicate a more severe and/or more specific phenotype. Color coding of AUTS2 syndrome severity scores is as follows: white, <7; light gray, 7–12; gray, 13–18; and dark gray, >18. See also Figure S2 and Table S7.

unclear whether they included an exon because of the limited resolution of the array. For these three individuals, we had no consent to perform further studies.

Overall, in our cohort of 49,684 affected individuals, we identified 24 persons (0.05%) harboring deletions disrupting the coding sequence. To assess the significance of this observation, we analyzed 16,784 controls from 12 cohorts by using arrays with high-density coverage of the *AUTS2* locus (Table S4). Although nine deletions were found, none of them disrupted an *AUTS2* exon (Table S6). The difference between exonic deletions in the cases (24/49,651) and those in controls (0/16,784) was highly significant ($p = 0.00092$), suggesting that exonic disruptions of *AUTS2* give rise to a highly penetrant phenotype in humans. This is supported by CNV data from the latest version of the Database of Genomic Variants (August 25, 2012), wherein none of the array-based studies show CNVs that disrupt an exon, and by the fact that none of the 24 probands with an exonic *AUTS2* deletion had a rare de novo CNV at another locus (Table S1).

We were able to obtain phenotypic data from 15 out of 24 probands with an exonic *AUTS2* deletion (cases 1–15), from the inversion case (16) and the translocation case (17) with one breakpoint in *AUTS2*, as well as from four family members carrying the familial *AUTS2* deletion. In these 17 probands, MLPA, FISH, high-density array CGH, and breakpoint sequencing confirmed the aberrations and further delineated the breakpoints. (Figure 1 and Table S1).

In total, 21 individuals from 17 families were included in our genotype-phenotype study (Table S7). In 8 (cases 5, 8, 10, 12, 14, 15, 16, and 17) out of 11 probands in which both parents were available for genetic testing, the *AUTS2* aberrations occurred de novo; the other three probands inherited the *AUTS2* deletion from an unaffected parent (case 1) or an affected parent (cases 4 and 6). In six probands (cases 2, 3, 7, 9, 11, and 13), the inheritance status of the *AUTS2* deletion could not be fully resolved because one or both parents were unavailable for testing. Of the ten individuals with an intragenic deletion (not including the first and last exon), four probands (cases 6, 7, 8, and 11) carried a deletion predicted to cause a frameshift, whereas the other six individuals (cases 1, 2, 3, 4, 9, and 10) carried in-frame deletions. Finally, in case 14, the deletion also included one downstream gene (*WBSCR17*), and in cases 13 and 15, the deletions also affected two downstream genes (*WBSCR17* and *CALN1*) (Figure 1, Table S7, and Figure S2).

Phenotypes

Next, we asked whether there were any recurrent phenotypic features associated with *AUTS2* disruptions. All 17 probands from whom detailed clinical data were available had ID and/or developmental delay; this had been the reason for diagnostic testing. One of the parents (the mother of case 4) carrying an *AUTS2* deletion had learning difficulties, one (the mother of case 6) had mild ID, and one (the father of case 1) had normal intelligence. Seven

Figure 2. Facial Characteristics of Cases with an *AUTS2* Aberration
(A) Case 1 at age 3 years shows no dysmorphic features.
(B and L) Front (B) and side (L) views of case 4 at age 2.5 years show a repaired cleft lip, mild proptosis, and short and mild upslanting palpebral fissures.
(C) The mother of case 4 shows a repaired cleft lip, ptosis, and retrognathia.
(D) Case 5 at age 3 years shows highly arched eyebrows, mild downslanting palpebral fissures, epicanthal folds, and a short philtrum.
(E, F, M, and N) Front (E) and side (M) views of case 6 at age 6 years. She is hypertelloric and has ptosis and downslanting palpebral fissures, a short philtrum, and a narrow mouth similarly to her brother, shown in (F) and (N) at the age of 10 years.
(G and O) Front (G) and side (O) views of case 9 at age 32 years show hypertelorism, proptosis, upslanting palpebral fissures, a short upturned philtrum, and a narrow mouth.
(H) Case 10 at age 2 years shows a prominent nasal tip, anteverted nares, and a short philtrum.
(I and P) Front (I) and side (P) views of case 13 at age 5.5 years show hypertelorism, ptosis, a broad nasal bridge, a short and upturned philtrum, and a narrow mouth.
(J, K, and Q) Case 15 at age 1 year (J) and 4.8 years (K and Q) shows a broad nasal bridge, short palpebral fissures and a short philtrum, and a narrow mouth. See also Table 1 and Table S7.

probands (cases 2, 5, 9, 12, 13, 16, and 17) were diagnosed with autism spectrum disorder or showed autistic behavior. In addition to the expected neurocognitive defects, we also observed a constellation of other recurrent clinical features in individuals with exonic deletions. These included microcephaly (14 individuals), short stature (12), feeding difficulties (10), hypotonia (8), and cerebral palsy (9). We also found recurrent dysmorphic features: hypertelorism (10), proptosis (6), ptosis (8), short palpebral fissures (8), epicanthal folds (7), a short and/or upturned philtrum (8), micrognathia (7), and a narrow mouth (12). Less frequent features were skeletal abnormalities including (signs of) arthrogryposis (3), umbilical or inguinal hernia (2), and heart defects (3) (Figure 2 and Table 1). The striking phenotypic complexity and variable size and position of the CNVs prompted us to evaluate the clinical information from the 17 probands and 4 family members carrying the familial *AUTS2* deletion included in this study to derive pathology scores on the basis of simple, objective criteria; we summarized these as the "AUTS2 syndrome severity score" (the maximum score is 32). Even though this paradigm is a crude approximation of the phenotypic diversity at this locus, we nonetheless observed dichotomization of phenotypes. Cases and family members 1–4, (all with 5′ in-frame deletions) scored significantly lower (median AUTS2 syndrome severity score = 5) than did cases (5–17) and family members with deletions of downstream exons, whole-gene deletions, or exons 1–4 deletions including the initiation codon (median AUTS2 syndrome severity score = 12) (Figures 1 and 3 and Table S7). This difference

Table 1. Clinical Features Characterizing the Individuals with AUTS2 Syndrome

Clinical Features	Cases	
	This Study (n/total)	Published (n/total)
General		
Age at examination	11 months to 32 years	3–16 years
Sex	13 female and 8 male	5 female and 4 male
De novo occurrence	9/13 (69%)	8/9 (89%)
Growth and Feeding		
Low birth weight	7/17 (41%)	2/8 (25%)
Short stature[a]	12/20 (60%)	4/9 (44%)
Microcephaly[b]	14/20 (70%)	1/6 (17%)
Feeding difficulties	10/21 (48%)	4/5 (80%)
Neurodevelopmental Features		
Intellectual disability and/or development delay	20/21 (95%)	9/9 (100%)
Autism or autistic behavior	7/21 (33%)	4/6 (67%)
Sound sensitivity	2/8 (25%)	2/4 (50%)
Hyperactivity and/or ADHD	3/21 (14%)	1/4 (25%)
Neurological Disorders		
Generalized hypotonia	8/21 (38%)	4/7 (57%)
Structural brain anomaly	3/11 (27%)	4/9 (44%)
Cerebral palsy and/or spasticity	9/21 (43%)	1/4 (25%)
Dysmorphic Features		
Highly arched eyebrows	8/21 (38%)	1/5 (20%)
Hypertelorism	10/21 (48%)	0/5 (0%)
Proptosis	6/21 (29%)	2/5 (40%)
Short palpebral fissures	8/21 (38%)	2/5 (40%)
Upslanting palpebral fissures	4/21 (19%)	1/5 (20%)
Ptosis	8/21 (38%)	2/5 (40%)
Epicanthal fold	7/21 (33%)	1/5 (20%)
Strabismus	5/21 (24%)	3/6 (50%)
Prominent nasal tip	5/21 (24%)	2/5 (40%)
Anteverted nares	3/21 (14%)	2/5 (40%)
Deep and/or broad nasal bridge	7/21 (33%)	1/5 (20%)
Short and/or upturned philtrum	8/21 (38%)	5/7 (71%)
Micrognathia and retrognatia	7/20 (35%)	2/5 (40%)
Low-set ears	6/20 (30%)	2/5 (40%)
Ear pit	2/20 (10%)	0/5 (0%)
Narrow mouth	12/21 (57%)	3/5 (60%)
Skeletal Abnormalities		
Kyphosis and/or scoliosis	2/9 (22%)	3/5 (60%)
Arthrogryposis and/or shallow palmar creases	3/20 (15%)	1/3 (33%)
Tight heel cords	5/8 (62%)	1/1 (100%)
Congenital Malformations		
Hernia umbilicalis and/or inguinalis	2/21 (9%)	1/9 (11%)
Patent foramen ovale and/or atrial septum defect	3/21 (14%)	1/9 (11%)

This table shows the frequency of clinical features in AUTS2 syndrome as the number of affected individuals with this feature (n) in relation to the total number of individuals for whom information was available for each feature (total). For a more detailed overview, see Table S7, which also includes an overview of cases described in the literature.[2–5]
[a]Short stature is defined as height below the tenth percentile.
[b]Microcephaly is defined as skull size below the second percentile.

was significant regardless of the inclusion or exclusion of affected family members ($p = 0.001$ or $p = 0.011$, respectively).

Detection of a C-Terminal *AUTS2* Isoform

The apparent dependence of severity scores on CNV location prompted us to evaluate the evolutionary conservation of each *AUTS2* exon (Figures S3 and S4); conservation was especially high in the 3′ gene region. Given the fact that the ENSEMBL annotation of the *AUTS2* sequences predicts the presence of several splice isoforms, we next looked for the presence of alternative isoforms in human brain mRNA. Using 5′ RACE, we identified a short 3′ *AUTS2* mRNA variant starting in the middle of exon 9, depicted in Figure 4. All transcripts detected employed the same start site (see also Figures S1C and S1D). The reading frame of the short transcript is identical to that of the full-length *AUTS2* transcript and is predicted to encode a polypeptide of 697 amino acids instead of the 1,259 amino acids of the full-length protein. The evolutionary conservation from humans to zebrafish suggests an important biological function for *AUTS2* and, together with the shorter transcript, gave us the opportunity to analyze the function of the C terminus of AUTS2 in a zebrafish model.

In Vivo Analysis of *AUTS2* in Zebrafish Embryos

Taken together, our CNV mapping data, our RACE analyses, and the strong correlation between phenotypic severity and position of the deletion suggest that the 3′ end of the *AUTS2* locus contains major functional elements that are encoded by both the full-length transcript and the shorter C-terminal isoform. Microcephaly is one of the most consistent clinical features in our cases (14/20; Table 1). We therefore asked whether AUTS2,

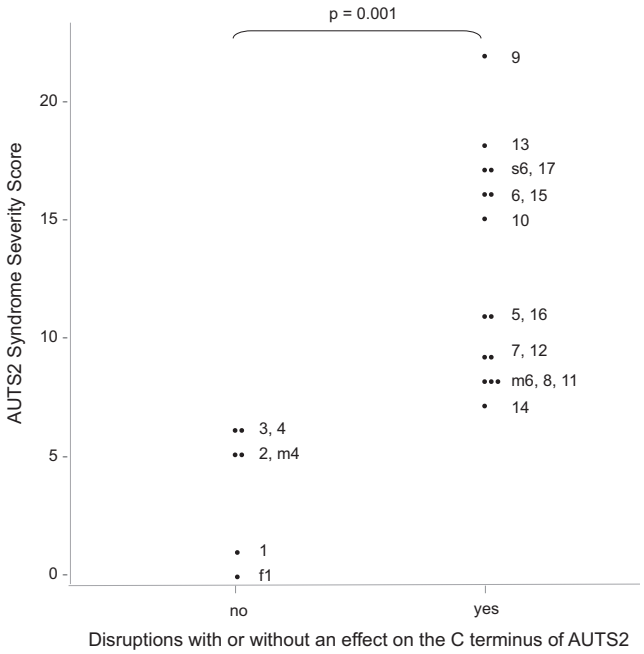

Figure 3. Scatter Plot of the AUTS2 Syndrome Severity Score for Disruptions Affecting the N or C Terminus of AUTS2
Scatter plot of the AUTS2 syndrome severity score for disruptions that affect the highly conserved amino acid sequence block encoded by exons 9–19 (yes) and the deletions not affecting this amino acid sequence (no) (see also Table S7 and Figure 4). The numbers refer to case numbers. The following abbreviations are used: f, father of patient x; m, mother of patient x; and s, sibling of patient x (see Table S7). The AUTS2 syndrome severity scores between these groups of cases differ significantly ($p = 0.001$, Kolmogorov-Smirnov Z test).

particularly the shorter C-terminal isoform, might be involved in the regulation of head size. Given that we have shown recently how head-size evaluations in zebrafish embryos can serve as a surrogate for the evaluation of candidate genes for neurocognitive traits,[21] we decided to create a zebrafish morphant for *auts2*. Using reciprocal BLAST, we identified a single *Danio rerio AUTS2* ortholog (*auts2* on chromosome 10; 62% amino acid identity and 72% similarity with the long isoform of *AUTS2*) (Figure 4A). We were able to detect endogenous *auts2* message by RT-PCR as early as embryonic 5-somite stage by using both 5′ and 3′ primer sets (data not shown). Next, we designed two splice-blocking morpholinos (sb-MOs): a 5′ MO targeting the splice donor site of exon 2 and a 3′ MO targeting the splice donor site of exon 10 (the 5′ and 3′ MOs were chosen to suppress the full-length transcript only and both *auts2* transcripts [if present], respectively; see Figure 4A and Figure S5). RT experiments demonstrated that both sb-MOs affected correct splicing of the *auts2* transcript (Figure S5). Masked scoring of embryos at 3 dpf showed a reproducible microcephaly phenotype—53% and 48% for 5′ and 3′ sb-MOs, respectively (Figures 5A and 5B)—that was concomitant with the efficiency of splice blocking of the two sb-MOs, as established by RT-PCR (Figure S5). The phenotype was unlikely to be driven by overall developmental delay; morphants had a normal appearance with regard to their pigment cells, there was no apparent pathology in other internal organs, such as the heart or the swim bladder, and their body length was indistinguishable from that of control embryos from the same clutch (Figure 5C). The phenotype was specific; the observed microcephaly caused by the two sb-MOs could be rescued efficiently with coinjection of wild-type human full-length mRNA (GenBank JQ670866) (Figures 5A and 5B). Strikingly, microcephalic embryos could also be rescued with the human short *AUTS2* isoform (GenBank JQ670867) in a manner indistinguishable from that with the full-length form, indicating that the observed phenotype is driven by sequences in exons 9–19. We also observed another recurrent dysmorphic feature in knockdown zebrafish morphants: micrognathia and retrognathia. To quantify this defect, we stained embryos injected with either a 5′ or 3′ sb-MO at 5 dpf with Alcian blue and performed quantitative morphometric analysis of the lower jaw. We observed a significant reduction of the distance between the Meckel and ceratohyal cartilages, indicating a reduced lower-jaw size comparable to the micrognathia and retrognathia seen in individuals with an *AUTS2* disruption (Figures 5D and 5E).

To probe the underlying cause(s) of the microcephalic phenotype further, we stained embryos at 2 dpf with antibodies against phosphohistone H3, an M phase marker, and HuC/D, a marker of postmitotic neurons.[22] This time point was selected because it precedes the development of microcephaly and, as such, allowed us to evaluate the forebrain prior to gross anatomical defects. We observed a striking reduction in phosphohistone-H3- and HuC/D-positive cells in embryos injected with either the 5′ or the 3′ MO, as well as loss of bilateral symmetry in HuC/D protein levels, indicating that the microcephaly phenotype is caused by disturbed neuronal proliferation. Both phenotypes could be rescued with the 3′ human mRNA (Figure 6).

Discussion

Our studies of 49,684 individuals with ID and/or MCAs revealed deletions in *AUTS2* in 44 individuals; at least 24 of these deletions involved exons. In contrast, we only found nine *AUTS2* deletions, none of which were exonic, in 16,784 controls, strongly indicating that intragenic *AUTS2* deletions that disrupt at least a portion of the coding sequence are a recurrent cause of neurodevelopmental defects in humans. The frequency of exonic deletions that we found was 1 in 2,000 cases, comparable with some of the recurrent deletions described by Cooper et al.,[12] such as the 10q23 deletion (*NRG3* [MIM 605533] and *GRID1* [MIM 610659]) and deletions causing Sotos syndrome (MIM 117550) or Rubinstein-Taybi syndrome (MIM 180849). This observed frequency is likely to be an

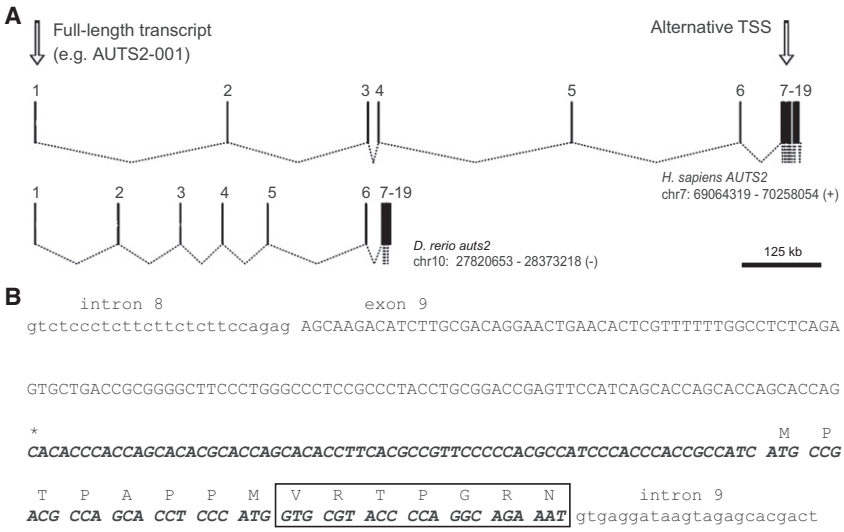

Figure 4. Exon Organization of *AUTS2* and Its Zebrafish Ortholog and Identification of a Novel Transcriptional Start Site in Exon 9 of Full-Length Human *AUTS2*

(A) Exon organization of *AUTS2* orthologs in humans and zebrafish. Arrows indicate two TSSs used in human brain mRNA. The alternative novel TSS is located 1.17 Mb downstream of the standard TSS in the cluster containing exons 7–19. Exons 1–6 (zebrafish) represent conserved sequences that are not annotated in the current zebrafish genome (for details, see Figure S4).

(B) Identification of an alternative *AUTS2* transcript detected in human brain mRNA by 5′ RACE. The alternative transcript starts in the center of exon 9 (asterisk) and contains the indicated cDNA sequence (in italics). The mRNA was spliced to exon 10 with the second of two known splice donor sites in exon 9, resulting in the incorporation of seven alternatively spliced amino acids (rectangle). The alternative mRNA uses the same reading frame as the conventional transcript. Conventional exons are in uppercase, and introns are in lowercase. See also Figures S1 and S3.

underestimate because smaller deletions (single-exon deletions and small indels within exons) and nonsense mutations are likely to cause AUTS2 syndrome and are missed with the techniques used here.

The individuals (cases 1–17) with an *AUTS2* aberration affecting the coding sequence studied here, together with previously reported cases, allowed us to delineate recurrent phenotypic features (ID, autism, microcephaly, mild short stature, feeding difficulties, hypotonia, cerebral palsy, and dysmorphic features) of the AUTS2 syndrome. Only 1 (the father of case 1) of the 21 persons studied in detail did not have any features of the AUTS2 syndrome, indicating a penetrance of around 95%. Although the phenotype of the AUTS2 syndrome is variable and the features are sometimes subtle, there are other examples where reverse genomics have shown variable phenotypes associated with the same locus.[23,24] Several lines of evidence support the causality of *AUTS2* deletions for this broad phenotypic spectrum; these are (1) the significant enrichment of exonic deletions in cases, (2) the fact that *auts2* zebrafish morphants show microcephaly and smaller lower-jaw size comparable to the human phenotype (these aberrant phenotypes can be fully rescued by both full-length and short 3′ human *AUTS2* transcript), (3) the fact that no individuals with an exonic deletion had a second rare de novo CNV, and (4) the fact that all exonic deletions were de novo or inherited from an affected parent except for the in-frame exon 2 deletion of case 1.

Individuals with in-frame exonic deletions in the 5′ part of the gene (exons 1–5) showed a milder phenotype mainly restricted to neurocognitive defects with no or limited dysmorphology or were normal, like the father of case 1. In contrast, deletions of the C-terminal part, encoded by both the short and full-length transcripts, cause a more severe phenotype including dysmorphology. This could potentially be related to the gene structure: because exons 7–19 are closely packed, deletions in this part of the gene often result in larger disruptions of the coding sequence. However, we also observed severe phenotypes in cases with small in-frame 3′ deletions, as well as in 3′ MO zebrafish, where the shorter 3′ transcript was sufficient to rescue the dysmorphology (microcephaly and smaller jaw size). This might suggest that the C-terminal part of the protein contains the crucial region for the observed dysmorphology. It is uncertain whether the shorter 3′ transcript is expressed at sufficiently high levels to explain the milder phenotype in humans with in-frame 5′ deletions. The milder phenotype might well be explained by the fact that *AUTS2* alleles with these deletions can still be transcribed and can thus result in a protein that contains the important C-terminal sequences.

In aggregate, our data indicate that *AUTS2* deletions, particularly when they involve the C terminus, give rise to a highly penetrant syndrome that includes neurocognitive defects. Our data highlight transcriptional complexity at the *AUTS2* locus and show that careful genomic, genetic, and functional dissection of such complexity can offer both clinical and mechanistic insights. Although little is known about the function(s) of AUTS2 or its isoforms, a role in neurodevelopment is suggested by the reduction of postmitotic neurons and loss of bilateral symmetry, which both might be driven by neurogenesis and/or migration defects in the zebrafish *auts2* morphants. The zebrafish model can be of great value for further studies of *AUTS2* function and can be helpful for defining the pathogenicity of specific genomic disruptions.

In conclusion, detailed analysis of the *AUTS2* locus allowed us to delineate a hitherto undescribed microdeletion

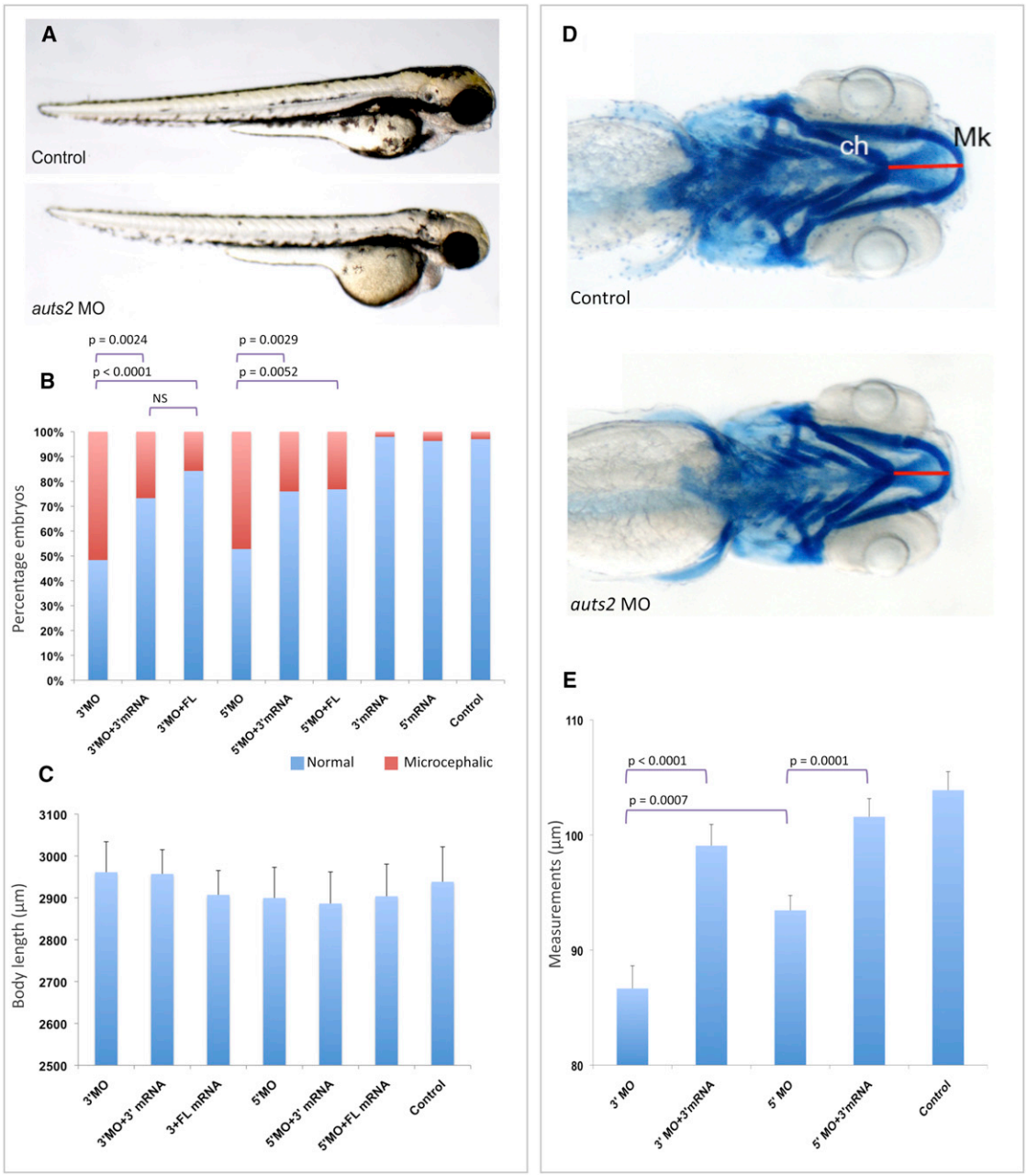

Figure 5. Suppression of *auts2* in Zebrafish Leads to Small Head Size and Craniofacial Defects
(A) Lateral views of representative control embryos and embryos injected with *auts2* MOs.
(B) Quantification of microcephaly was performed in embryo batches injected with 4.5 ng 5′ MO (targeting exon 2 donor splice) or 6 ng 3′ MO (targeting exon 10 donor splice) plus 100 pg wild-type human *AUTS2* full-length (FL) or short isoform (3′) mRNAs (n = 56–91 embryos per injection). p values are denoted on the bar graph. The following abbreviation is used: NS, nonsignificant.
(C) No significant difference in body length was observed in *auts2* morphants and rescued embryos at 2 dpf. Bars represent the average length of 30 embryos, which were scored blindly to injection cocktail. Data are shown as the mean ± SD.
(D) Ventral views of representative control embryos and those injected with *auts2* MOs (either a 3′ or 5′ MO) at 5 dpf. Cartilage structures were visualized by whole-mount Alcian-blue staining at 5 dpf, allowing measurement of the distance between ceratohyal and Meckel's cartilages (red lines).
(E) Averaged distance measurements are presented as the mean ± SEM. The corresponding p values are denoted on the bar graph (two-tailed t test comparisons). The following abbreviations are used: ch, ceratohyal cartilage; and Mk, Meckel's cartilage.

syndrome occurring with a frequency that approximates the frequency of deletions causing Sotos syndrome or Rubinstein-Taby syndrome.[12] This AUTS2 syndrome has presumably remained undescribed because (1) the specific characteristics of the resulting phenotype are subtle, (2) the severity of the syndrome is highly variable, and (3) the penetrance is dependent on location and type of deletion.

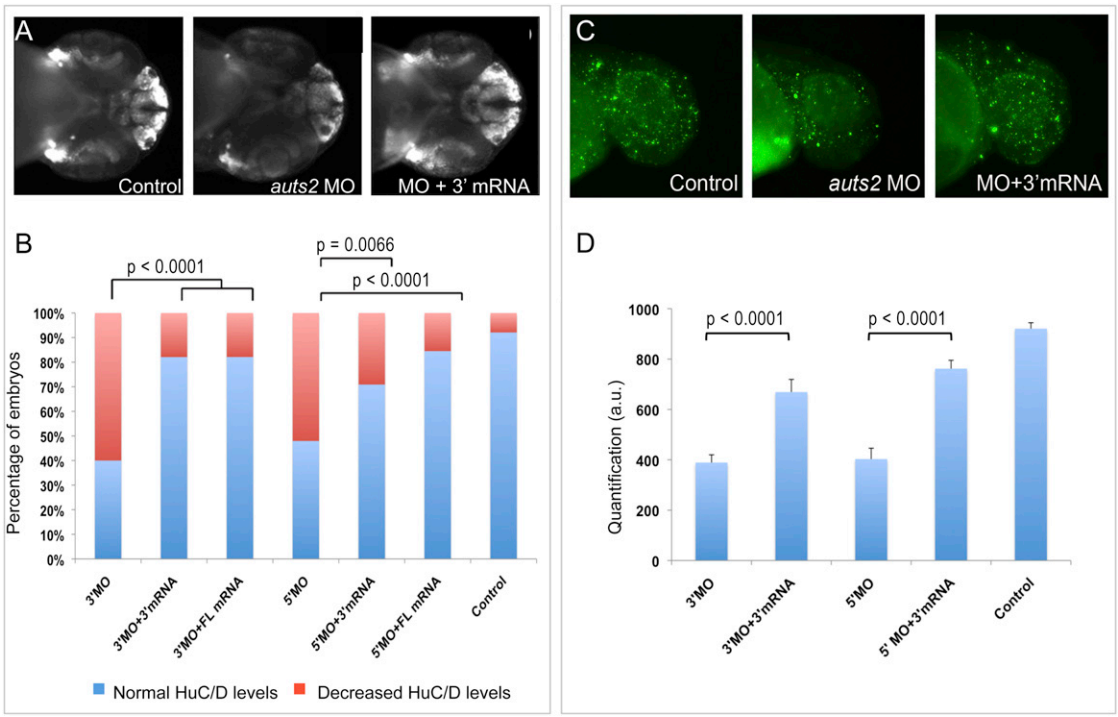

Figure 6. Suppression of *auts2* Leads to Reduced HuC/D Protein Levels and Fewer Proliferating Cells
(A) Suppression of *auts2* leads to a decrease of HuC/D levels at 2 dpf. Representative photographs (with HuC/D-antibody staining) show the ventral views of a control, an embryo injected with an *auts2* MO, and a rescued embryo injected with an *auts2* MO plus 3′ human *AUTS2* mRNA at 2 dpf. HuC/D levels in the anterior forebrain of the embryo injected with the *auts2* MO are considerably lower than those of the control embryo. This defect was rescued significantly by coinjection of full-length (FL) or short isoform (3′) human *AUTS2* mRNAs.
(B) Percentage of embryos with normal, bilateral HuC/D protein levels in the anterior forebrain (blue) or decreased and/or unilateral HuC/D protein levels (red) in embryo batches injected with *auts2* MOs alone or MOs plus human *AUTS2* FL or 3′ mRNA (MO + 3′ mRNA). p values are denoted on the bar graph.
(C) Phosphohistone-H3 staining for proliferating cells in the zebrafish brain at 2 dpf.
(D) Quantification of phosphohistone-H3-staining intensities from 20 embryos each (control embryos or embryos injected with MOs alone or MOs plus 3′ or 5′ human *AUTS2* mRNA). Data are represented as the mean ± SEM. The corresponding p values are denoted on the bar graph (two-tailed t test comparisons between MO-injected and rescued embryos).

Supplemental Data

Supplemental Data include five figures and seven tables and can be found with this article online at http://www.cell.com/AJHG.

Acknowledgments

The authors would like to thank all patients and their families for their major contribution; without them, we would not have been able to describe this syndrome. We thank Marjolein van de Mespel, Desiree Linders, Stefan Strijbis, Amanda Clarkson, and Carrie Hanscom for their contribution to the laboratory work in this project and Shahrin Pereira for clinical coordination. This study made use of data generated by the Wellcome Trust Case Control Consortium. A full list of the investigators who contributed to the generation of the data is available at www.wtccc.org.uk. Funding for this project was provided by the Wellcome Trust under awards 076113 and 085475, as well as by the National Institutes of Health (GM061354, HD065286, and MH095867), the American Heart Association (11POST7160006), and a Distinguished Brumley Professorship to N.K. Evan Eichler is a Howards Hughes Medical Institute investigator. The authors thank Klaas Kok for making available the control data of The Low-Lands Consortium for this study and for developing the custom design of the 180K Agilent oligo array used in The Netherlands. We acknowledge Soheil Shams from Bio-Discovery for his help with processing the different array data files. J.A.R. and N.J.N. are employees of Signature Genomic Laboratories, a subsidiary of PerkinElmer, and E.E.E. is on the scientific advisory boards for Pacific Biosciences, SynapDx, and DNAnexus.

Received: September 14, 2012
Revised: October 6, 2012
Accepted: December 20, 2012
Published: January 17, 2013

Web Resources

The URLs for the data presented herein are as follows:

BLAST, http://blast.ncbi.nlm.nih.gov/
DECIPHER, http://decipher.sanger.ac.uk/
DGV (Database of Genomic Variants), http://projects.tcag.ca/cgi-bin/variation/gbrowse/hg18/#search
Gene Expression Omnibus, http://www.ncbi.nlm.nih.gov/geo/
HapMap, http://hapmap.ncbi.nlm.nih.gov/downloads/raw_data/hapmap3_affy6.0/
Online Mendelian Inheritance in Man (OMIM), http://www.omim.org/
Wellcome Trust Case Control Consortium 2, https://www.wtccc.org.uk/ccc2/

Accession Numbers

The Gene Expression Omnibus accession numbers for the microarray data, the nucleotide sequence of the full-length human *AUTS2* transcript, and the nucleotide sequence of the shorter 3′ alternative human *AUTS2* transcript reported in this paper are GSE37657, JQ670866, and JQ670867, respectively.

References

1. Sultana, R., Yu, C.E., Yu, J., Munson, J., Chen, D., Hua, W., Estes, A., Cortes, F., de la Barra, F., Yu, D., et al. (2002). Identification of a novel gene on chromosome 7q11.2 interrupted by a translocation breakpoint in a pair of autistic twins. Genomics *80*, 129–134.
2. Huang, X.L., Zou, Y.S., Maher, T.A., Newton, S., and Milunsky, J.M. (2010). A de novo balanced translocation breakpoint truncating the autism susceptibility candidate 2 (*AUTS2*) gene in a patient with autism. Am. J. Med. Genet. A. *152A*, 2112–2114.
3. Kalscheuer, V.M., FitzPatrick, D., Tommerup, N., Bugge, M., Niebuhr, E., Neumann, L.M., Tzschach, A., Shoichet, S.A., Menzel, C., Erdogan, F., et al. (2007). Mutations in autism susceptibility candidate 2 (*AUTS2*) in patients with mental retardation. Hum. Genet. *121*, 501–509.
4. Bakkaloglu, B., O'Roak, B.J., Louvi, A., Gupta, A.R., Abelson, J.F., Morgan, T.M., Chawarska, K., Klin, A., Ercan-Sencicek, A.G., Stillman, A.A., et al. (2008). Molecular cytogenetic analysis and resequencing of contactin associated protein-like 2 in autism spectrum disorders. Am. J. Hum. Genet. *82*, 165–173.
5. Nagamani, S.C., Erez, A., Ben-Zeev, B., Frydman, M., Winter, S., Zeller, R., El-Khechen, D., Escobar, L., Stankiewicz, P., Patel, A., and Wai Cheung, S. (2012). Detection of copy-number variation in *AUTS2* gene by targeted exonic array CGH in patients with developmental delay and autistic spectrum disorders. Eur. J. Hum. Genet. Published online August 8, 2012. http://dx.doi.org/10.1038/ejhg.2012.157.
6. Mefford, H.C., Muhle, H., Ostertag, P., von Spiczak, S., Buysse, K., Baker, C., Franke, A., Malafosse, A., Genton, P., Thomas, P., et al. (2010). Genome-wide copy number variation in epilepsy: Novel susceptibility loci in idiopathic generalized and focal epilepsies. PLoS Genet. *6*, e1000962.
7. Firth, H.V., Richards, S.M., Bevan, A.P., Clayton, S., Corpas, M., Rajan, D., Van Vooren, S., Moreau, Y., Pettett, R.M., and Carter, N.P. (2009). DECIPHER: Database of Chromosomal Imbalance and Phenotype in Humans Using Ensembl Resources. Am. J. Hum. Genet. *84*, 524–533.
8. Talkowski, M.E., Ernst, C., Heilbut, A., Chiang, C., Hanscom, C., Lindgren, A., Kirby, A., Liu, S., Muddukrishna, B., Ohsumi, T.K., et al. (2011). Next-generation sequencing strategies enable routine detection of balanced chromosome rearrangements for clinical diagnostics and genetic research. Am. J. Hum. Genet. *88*, 469–481.
9. Talkowski, M.E., Mullegama, S.V., Rosenfeld, J.A., van Bon, B.W., Shen, Y., Repnikova, E.A., Gastier-Foster, J., Thrush, D.L., Kathiresan, S., Ruderfer, D.M., et al. (2011). Assessment of 2q23.1 microdeletion syndrome implicates MBD5 as a single causal locus of intellectual disability, epilepsy, and autism spectrum disorder. Am. J. Hum. Genet. *89*, 551–563.
10. Talkowski, M.E., Rosenfeld, J.A., Blumenthal, I., Pillalamarri, V., Chiang, C., Heilbut, A., Ernst, C., Hanscom, C., Rossin, E., Lindgren, A.M., et al. (2012). Sequencing chromosomal abnormalities reveals neurodevelopmental loci that confer risk across diagnostic boundaries. Cell *149*, 525–537.
11. Conrad, D.F., Pinto, D., Redon, R., Feuk, L., Gokcumen, O., Zhang, Y., Aerts, J., Andrews, T.D., Barnes, C., Campbell, P., et al.; Wellcome Trust Case Control Consortium. (2010). Origins and functional impact of copy number variation in the human genome. Nature *464*, 704–712.
12. Cooper, G.M., Coe, B.P., Girirajan, S., Rosenfeld, J.A., Vu, T.H., Baker, C., Williams, C., Stalker, H., Hamid, R., Hannig, V., et al. (2011). A copy number variation morbidity map of developmental delay. Nat. Genet. *43*, 838–846.
13. Altshuler, D.M., Gibbs, R.A., Peltonen, L., Altshuler, D.M., Gibbs, R.A., Peltonen, L., Dermitzakis, E., Schaffner, S.F., Yu, F., Peltonen, L., et al.; International HapMap 3 Consortium. (2010). Integrating common and rare genetic variation in diverse human populations. Nature *467*, 52–58.
14. Lionel, A.C., Crosbie, J., Barbosa, N., Goodale, T., Thiruvahindrapuram, B., Rickaby, J., Gazzellone, M., Carson, A.R., Howe, J.L., Wang, Z., et al. (2011). Rare copy number variation discovery and cross-disorder comparisons identify risk genes for ADHD. Sci. Transl. Med. *3*, 95ra75.
15. Pinto, D., Darvishi, K., Shi, X., Rajan, D., Rigler, D., Fitzgerald, T., Lionel, A.C., Thiruvahindrapuram, B., Macdonald, J.R., Mills, R., et al. (2011). Comprehensive assessment of array-based platforms and calling algorithms for detection of copy number variants. Nat. Biotechnol. *29*, 512–520.
16. Oeseburg, B., Dijkstra, G.J., Groothoff, J.W., Reijneveld, S.A., and Jansen, D.E. (2011). Prevalence of chronic health conditions in children with intellectual disability: a systematic literature review. Intellect. Dev. Disabil. *49*, 59–85.
17. Edgar, R.C. (2004). MUSCLE: Multiple sequence alignment with high accuracy and high throughput. Nucleic Acids Res. *32*, 1792–1797.
18. Altschul, S.F., Madden, T.L., Schäffer, A.A., Zhang, J., Zhang, Z., Miller, W., and Lipman, D.J. (1997). Gapped BLAST and PSI-BLAST: A new generation of protein database search programs. Nucleic Acids Res. *25*, 3389–3402.
19. Leitch, C.C., Zaghloul, N.A., Davis, E.E., Stoetzel, C., Diaz-Font, A., Rix, S., Alfadhel, M., Lewis, R.A., Eyaid, W., Banin, E., et al. (2008). Hypomorphic mutations in syndromic encephalocele genes are associated with Bardet-Biedl syndrome. Nat. Genet. *40*, 443–448.
20. Rooryck, C., Diaz-Font, A., Osborn, D.P., Chabchoub, E., Hernandez-Hernandez, V., Shamseldin, H., Kenny, J., Waters, A., Jenkins, D., Kaissi, A.A., et al. (2011). Mutations in lectin complement pathway genes COLEC11 and MASP1 cause 3MC syndrome. Nat. Genet. *43*, 197–203.
21. Golzio, C., Willer, J., Talkowski, M.E., Oh, E.C., Taniguchi, Y., Jacquemont, S., Reymond, A., Sun, M., Sawa, A., Gusella, J.F., et al. (2012). KCTD13 is a major driver of mirrored neuroanatomical phenotypes of the 16p11.2 copy number variant. Nature *485*, 363–367.
22. Grandel, H., Kaslin, J., Ganz, J., Wenzel, I., and Brand, M. (2006). Neural stem cells and neurogenesis in the adult zebrafish brain: Origin, proliferation dynamics, migration and cell fate. Dev. Biol. *295*, 263–277.
23. Deak, K.L., Horn, S.R., and Rehder, C.W. (2011). The evolving picture of microdeletion/microduplication syndromes in the age of microarray analysis: Variable expressivity and genomic complexity. Clin. Lab. Med. *31*, 543–564, viii.
24. van Bon, B.W., Koolen, D.A., Brueton, L., McMullan, D., Lichtenbelt, K.D., Adès, L.C., Peters, G., Gibson, K., Moloney, S., Novara, F., et al. (2010). The 2q23.1 microdeletion syndrome: Clinical and behavioural phenotype. Eur. J. Hum. Genet. *18*, 163–170.